Modelling Brain Atrophy Dynamics Enhances Predicting Cognitive Decline in Alzheimer's Disease Continuum

Wooseok Jung (wooseok.jung@vuno.co)
R&D Centre, VUNO Inc.
479 Gangnam-daero, Seoul, South Korea, 06541

Saehyun Kim (saehyun.kim@vuno.co)
R&D Centre, VUNO Inc.
479 Gangnam-daero, Seoul, South Korea, 06541

Dong-Hee Kim (donghee.kim@vuno.co)
R&D Centre, VUNO Inc.
479 Gangnam-daero, Seoul, South Korea, 06541

Won Hwa Kim (wonhwa@postech.ac.kr)
POSTECH
Pohang, South Korea

Abstract

Alzheimer's disease (AD) is recognized as a continuum of cognitive decline with underlying biological changes, and predicting the disease progression is crucial. Brain atrophy status obtained from volumetric MRI is pivotal for assessing disease severity and prognosis during the continuum, but modelling its longitudinal change and its relationship with the progression has been underexplored. This study proposes a novel deep learning-based method that precisely models the atrophy dynamics across 62 cortical and subcortical regions of mild cognitive impairment (MCI) subjects collected from the ADNI database, followed by a unique training scheme to add the effects of beta-amyloid protein deposition on atrophy and to model subject-specific dynamical features. Furthermore, we directly implement the dynamics into the MCI to dementia conversion prediction task. Our findings demonstrate the feasibility of modelling atrophy dynamics using deep learning and suggest that leveraging dynamics representation (DR) enhances the conversion prediction.

Keywords: Brain atrophy dynamics; Neural DE solver; Mild cognitive impairment due to Alzheimer's disease

Introduction

Alzheimer's disease (AD), the most prevalent form of dementia, is now understood as a continuum spanning a preclinical AD stage with underlying pathophysiological developments to stages with severe cognitive decline (Aisen et al., 2017). Mild cognitive impairment (MCI) due to AD represents an earlier stage in this continuum, characterised by cognitive deficits that do not significantly affect daily functioning. Studies indicate that up to 50% of individuals with MCI due to AD progress to Alzheimer's dementia within a decade (Liss et al., 2021). This underscores the importance of accurate progression prediction, particularly in light of recently introduced anti-amyloid therapies (Van Dyck et al., 2023).

Extensive research has leveraged volumetric MRI to extract brain atrophy features and construct machine learning models for predicting disease progression (Y. Chen et al., 2022). Notably, reduced baseline hippocampal volume and its faster reduction have been identified as significant risk factors for the conversion (Tabatabaei-Jafari et al., 2019). Nevertheless, previous studies have assessed volume changes of different regions independently at a high level, rather than systematically modelling the interrelated dynamics of atrophy across several brain regions. This limitation motivates a novel perspective: viewing brain atrophy as a dynamical system.

In this research, we first introduce an ordinary differential equation (ODE) with learnable parameters to model the brain atrophy dynamics and apply a two-stage training scheme to fit the parameters subject-wisely. Furthermore, we exploit the dynamics to improve the accuracy of predicting conversion to dementia by directly implementing them as input features. To the best of our knowledge, this is the first work to computationally define atrophy rates and elucidate the effects of amyloid pathology on brain atrophy progression with a neural ODE.

Materials and Methods

Dataset

The study utilised 2,292 3T 3D T1-weighted volumetric brain MRI scans of individuals with mild cognitive impairment (MCI) from the Alzheimer's Disease Neuroimaging Initiative (ADNI) database (`adni.loni.usc.edu`). All subjects had at least two years of follow-up MRI data. Subjects were classified as progressive MCI (pMCI, n = 63, Global CDR score increased from 0.5 to 1 within 3 years) or static MCI (sMCI, n = 308, CDR remained 0.5) (Albert et al., 2013). To investigate the amyloid effect on brain atrophy progression, baseline average 18F-AV45 amyloid positron emission tomography (PET) standardised uptake value ratios (SUVRs) in the frontoparietal cortices were used (Landau et al., 2013).

Brain Atrophy Dynamics

Atrophy Quantification All MRI scans were registered to the corresponding subject's baseline scan initially. We leveraged skull stripping and whole brain segmentation algorithms to obtain volumes of 62 cortical and subcortical regions accurately (C. Suh et al., 2020; P. S. Suh et al., 2023). Then, the residual intracranial volume adjustment was performed to minimise volume changes due to head size differences (Voevodskaya et al., 2014). Finally, by comparing the volumes to age- and sex-matched cognitively normal (CN) individuals from the ADNI database, we acquired normative percentile (NP) values representing the cumulative distribution of Gaussian random variables with mean and variance derived from the normative data (Figure 1). Hence, lower NP values indicate smaller volumes compared to normal populations, designating greater atrophy. This procedure effectively quantified the regional brain atrophy across subjects.

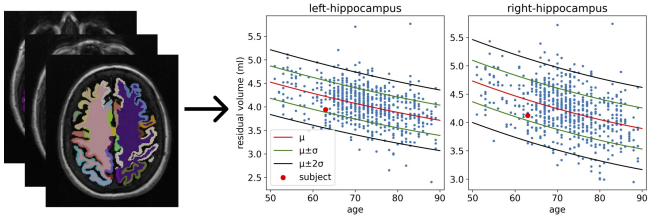

Figure 1: Atrophy Quantification Pipeline for 3D T1 MR Scans: (1) whole brain segmentation to obtain volumes of 62 cortical and subcortical regions (2) NPs to rank the subject's regional volumes compared to CN population. Examples of computing bilateral hippocampal atrophies are illustrated.

Modelling the Dynamics We assumed that the longitudinal NP change since (t_0) is governed by the following linear ODE:

$$\frac{d\mathbf{p}^{(j)}}{dt} = A^{(j)}\mathbf{p}^{(j)} + \beta^{(j)}\mathbf{a}, \;\; \mathbf{p}(t) = \mathbf{p}(t_0) + \int_{t_0}^{t} \mathbf{p}'(\tau)d\tau. \quad (1)$$

Here $\mathbf{p}^{(j)}$ represents the NP values of subject j, $A^{(j)}$ is a subject-specific linear neural representation (LNR) of atrophy dynamics showing correlations between regions during atrophy progression, whose precise definition will be provided

shortly. To consider the beta-amyloid effect on brain atrophy, the amyloid SUVR term $\beta^{(j)}$ multiplied by a learnable parameter vector **a** which is assumed to be constant across subjects.

To derive the LNR $A^{(j)}$, we initially trained the ODE across all subjects to identify the optimal **a**. This step accounted for the variability in sampling timeframes across subjects by approximating the ground truth NP values as a series of linear equations that have y-intercept at $\mathbf{p}(t_0)$ (Figure 2), facilitating batch-wise training of the ODE. Subsequently, by freezing **a** and initializing $A^{(j)}$ by the resulting value from the first stage, we trained the ODEs on each subject's NP data to ensure that $A^{(j)}$s precisely mirrored individual patterns.

Dementia Conversion Prediction

To evaluate the predictive capacity of the atrophy dynamics for MCI to dementia conversion, we trained a deep learning network which utilizes the LNR $A^{(j)}$ and amyloid-beta SUVR $\beta^{(j)}$ as input variables (Figure 2). To benchmark our approach, we established two baseline comparisons: one using only the amyloid-beta information for classification, and another using a neural network with baseline normative percentile vectors instead of $A^{(j)}$s. We investigated if the representation of atrophy dynamics derived from our method combined with beta-amyloid deposition yields more significant insights into the conversion from MCI to dementia, surpassing the predictive capabilities of traditional amyloid classification and approaches relying solely on baseline volumetry results.

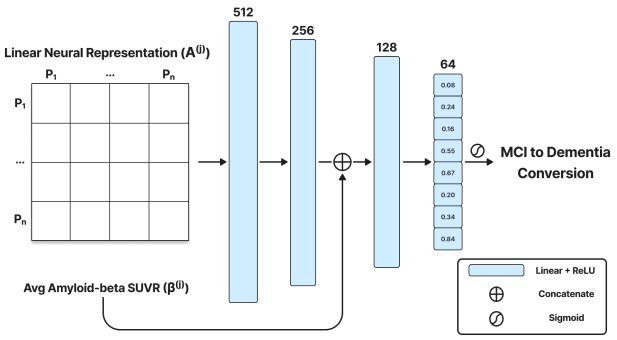

Figure 2: A small neural network to predict MCI to dementia conversion from neural representations of atrophy dynamics.

Results

We leveraged an efficient ODE-solving method from the Torchdiffeq library (R. T. Q. Chen, 2018) to model the atrophy dynamics. After the two-stage training, we observed sharper declines of normative percentiles in pMCI subjects, even if baseline NPs were similar to those of sMCI subjects, as expected. Specifically, the right entorhinal cortex, right middle temporal gyrus, and right inferior parietal gyrus showed statistically greater ($p < .05$) decline rates between pMCI and sMCI patients in terms of the diagonal entries of $A^{(j)}$. Figure 3 illustrates normative percentiles of those regions. The large overlapping of NP progression between sMCI and pMCI groups implies considering atrophy status only could make distinguishing the conversion group difficult. Also, training the atrophy dynamics only with the first stage was insufficient to capture subject-specific atrophy patterns (table 1).

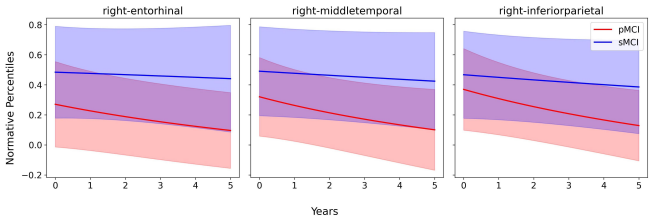

Figure 3: Prediction results of the atrophy dynamics model after applying the two-stage training scheme. Predicted normative percentile changes of three different conversion-related regions of sMCI (blue) and pMCI (red) patients are plotted.

Table 1: Prediction vs Ground Truth Mean Absolute Error

Region	Stage 1	Stage 2
right-entorhinal	0.1	0.032
right-middletemporal	0.075	0.03
right-inferiorparietal	0.08	0.032

In the conversion prediction task, using amyloid values alone yielded high sensitivity but low specificity, implying that many amyloid-positive MCI subjects did not progress to dementia (table 2). Integrating baseline (Bl) NPs with amyloid substantially improved specificity at the cost of reduced sensitivity. Sensitivity was recovered with increased AUROC when the linear neural representations (LNRs) of the atrophy dynamics were instead leveraged but reduced specificity.

Table 2: MCI to Dementia Conversion Prediction Results

Model Input	Sensitivity	Specificity	AUROC
Amyloid only[1]	0.891	0.548	N/A
Amyloid + Bl NPs	0.759	0.735	0.753
Amyloid + LNRs	0.891	0.681	0.780

Conclusion

This study introduced a novel approach to accurately model brain atrophy dynamics across cortical and subcortical regions in subjects along the Alzheimer's disease continuum. Leveraging subject-specific dynamics with amyloid SUVR accurately predicted MCI to dementia conversion. A notable limitation of this work is the assumption of a linear ODE structure, which may not fully capture the neurodegeneration's complex, nonlinear nature. Most importantly, the proposed atrophy dynamics cannot be modelled without a tracked record of MRI scans, preventing real-world application of this method. Hence, considering white matter connectivity obtained from diffusion tensor imaging at baseline might be desired to construct more robust dynamics. Future research should also examine integrating tauopathy information or using region-specific amyloid SUVR instead of the average SUVR to elaborate on how pathophysiological changes lead to regional neuron losses theoretically.

[1] Cut-off of 1.11 applied (Joshi et al., 2012).

Acknowledgments

We appreciate Renaud Lambiotte for providing feedback on the preliminary version of the atrophy dynamics model. Data used in the preparation of this article were obtained from the Alzheimer's Disease Neuroimaging Initiative (ADNI) database (`adni.loni.usc.edu`). As such, the investigators within the ADNI contributed to the design and implementation of ADNI and/or provided data but did not participate in the analysis or writing of this report. Data collection method and data platform used in this project was funded by the Alzheimer's Disease Neuroimaging Initiative (ADNI) (National Institutes of Health Grant U01 AG024904) and DOD ADNI (Department of Defense award number W81XWH-12-2-0012).

References

Aisen, P. S., Cummings, J., Jack, C. R., Morris, J. C., Sperling, R., Frölich, L., ... others (2017). On the path to 2025: understanding the alzheimer's disease continuum. *Alzheimer's research & therapy*, *9*, 1–10.

Albert, M. S., DeKosky, S. T., Dickson, D., Dubois, B., Feldman, H. H., Fox, N. C., ... others (2013). The diagnosis of mild cognitive impairment due to alzheimer's disease: recommendations from the national institute on aging-alzheimer's association workgroups on diagnostic guidelines for alzheimer's disease. *Focus*, *11*(1), 96–106.

Chalnick, A., & Billman, D. (1988). Unsupervised learning of correlational structure. In *Proceedings of the tenth annual conference of the cognitive science society* (pp. 510–516). Hillsdale, NJ: Lawrence Erlbaum Associates.

Chen, R. T. Q. (2018). *torchdiffeq.* Retrieved from `https://github.com/rtqichen/torchdiffeq`

Chen, Y., Qian, X., Zhang, Y., Su, W., Huang, Y., Wang, X., ... Ma, Y. (2022). Prediction models for conversion from mild cognitive impairment to alzheimer's disease: A systematic review and meta-analysis. *Frontiers in Aging Neuroscience*, *14*, 840386.

Feigenbaum, E. A. (1963). The simulation of verbal learning behavior. In E. A. Feigenbaum & J. Feldman (Eds.), *Computers and thought.* New York: McGraw-Hill.

Hill, J. A. C. (1983). A computational model of language acquisition in the two-year old. *Cognition and Brain Theory*, *6*, 287–317.

Joshi, A. D., Pontecorvo, M. J., Clark, C. M., Carpenter, A. P., Jennings, D. L., Sadowsky, C. H., ... others (2012). Performance characteristics of amyloid pet with florbetapir f 18 in patients with alzheimer's disease and cognitively normal subjects. *Journal of Nuclear Medicine*, *53*(3), 378–384.

Landau, S. M., Lu, M., Joshi, A. D., Pontecorvo, M., Mintun, M. A., Trojanowski, J. Q., ... Initiative, A. D. N. (2013). Comparing positron emission tomography imaging and cerebrospinal fluid measurements of β-amyloid. *Annals of neurology*, *74*(6), 826–836.

Liss, J., Seleri Assunção, S., Cummings, J., Atri, A., Geldmacher, D., Candela, S., ... others (2021). Practical recommendations for timely, accurate diagnosis of symptomatic alzheimer's disease (mci and dementia) in primary care: a review and synthesis. *Journal of internal medicine*, *290*(2), 310–334.

Matlock, T. (2001). *How real is fictive motion?* Doctoral dissertation, Psychology Department, University of California, Santa Cruz.

Newell, A., & Simon, H. A. (1972). *Human problem solving*. Englewood Cliffs, NJ: Prentice-Hall.

Ohlsson, S., & Langley, P. (1985). *Identifying solution paths in cognitive diagnosis* (Tech. Rep. No. CMU-RI-TR-85-2). Pittsburgh, PA: Carnegie Mellon University, The Robotics Institute.

Shrager, J., & Langley, P. (Eds.). (1990). *Computational models of scientific discovery and theory formation*. San Mateo, CA: Morgan Kaufmann.

Suh, C., Shim, W., Kim, S., Roh, J., Lee, J.-H., Kim, M.-J., ... others (2020). Development and validation of a deep learning–based automatic brain segmentation and classification algorithm for alzheimer disease using 3d t1-weighted volumetric images. *American Journal of Neuroradiology*, *41*(12), 2227–2234.

Suh, P. S., Jung, W., Suh, C. H., Kim, J., Oh, J., Heo, H., ... others (2023). Development and validation of a deep learning-based automatic segmentation model for assessing intracranial volume: comparison with neuroquant, freesurfer, and synthseg. *Frontiers in Neurology*, *14*, 1221892.

Tabatabaei-Jafari, H., Shaw, M. E., Walsh, E., Cherbuin, N., (ADNI, A. D. N. I., et al. (2019). Regional brain atrophy predicts time to conversion to alzheimer's disease, dependent on baseline volume. *Neurobiology of aging*, *83*, 86–94.

Van Dyck, C. H., Swanson, C. J., Aisen, P., Bateman, R. J., Chen, C., Gee, M., ... others (2023). Lecanemab in early alzheimer's disease. *New England Journal of Medicine*, *388*(1), 9–21.

Voevodskaya, O., Simmons, A., Nordenskjöld, R., Kullberg, J., Ahlström, H., Lind, L., ... Initiative, A. D. N. (2014). The effects of intracranial volume adjustment approaches on multiple regional mri volumes in healthy aging and alzheimer's disease. *Frontiers in aging neuroscience*, *6*, 264.